

# $\beta_3$ adrenergic receptor in the kidney may be a new player in sympathetic regulation of renal function

OPEN

Giuseppe Procino<sup>1,7</sup>, Monica Carmosino<sup>2,7</sup>, Serena Milano<sup>1</sup>, Massimo Dal Monte<sup>3</sup>, Giorgia Schena<sup>2</sup>, Maria Mastrodonato<sup>4</sup>, Andrea Gerbino<sup>1</sup>, Paola Bagnoli<sup>3</sup> and Maria Svelto<sup>1,5,6</sup>

<sup>1</sup>Department of Biosciences, Biotechnologies and Biopharmaceutics, University of Bari, Bari, Italy; <sup>2</sup>Department of Sciences, University of Basilicata, Potenza, Italy; <sup>3</sup>Department of Biology, University of Pisa, Pisa, Italy; <sup>4</sup>Department of Biology, University of Bari, Bari, Italy; <sup>5</sup>Institute of Biomembranes and Bioenergetics, National Research Council, Bari, Italy; and <sup>6</sup>National Institute of Biostructures and Biosystems (INBB), Rome, Italy

To date, the study of the sympathetic regulation of renal function has been restricted to the important contribution of  $\beta_1$ - and  $\beta_2$ -adrenergic receptors (ARs). Here we investigate the expression and the possible physiologic role of  $\beta_3$ -adrenergic receptor ( $\beta_3$ -AR) in mouse kidney. The  $\beta_3$ -AR is expressed in most of the nephron segments that also express the type 2 vasopressin receptor (AVPR2), including the thick ascending limb and the cortical and outer medullary collecting duct. *Ex vivo* experiments in mouse kidney tubules showed that  $\beta_3$ -AR stimulation with the selective agonist BRL37344 increased intracellular cAMP levels and promoted 2 key processes in the urine concentrating mechanism. These are accumulation of the water channel aquaporin 2 at the apical plasma membrane in the collecting duct and activation of the Na-K-2Cl symporter in the thick ascending limb. Both effects were prevented by the  $\beta_3$ -AR antagonist L748,337 or by the protein kinase A inhibitor H89. Interestingly, genetic inactivation of  $\beta_3$ -AR in mice was associated with significantly increased urine excretion of water, sodium, potassium, and chloride. Stimulation of  $\beta_3$ -AR significantly reduced urine excretion of water and the same electrolytes. Moreover, BRL37344 promoted a potent antidiuretic effect in AVPR2-null mice. Thus, our findings are of potential physiologic importance as they uncover the antidiuretic effect of  $\beta_3$ -AR stimulation in the kidney. Hence,  $\beta_3$ -AR agonism might be useful to bypass AVPR2-inactivating mutations.

*Kidney International* (2016) ■, ■-■; <http://dx.doi.org/10.1016/j.kint.2016.03.020>

KEYWORDS: antidiuresis; AQP2;  $\beta_3$  adrenergic receptors; NKCC2; vasopressin  
Copyright © 2016, International Society of Nephrology. Published by Elsevier Inc. This is an open access article under the CC BY-NC-ND license (<http://creativecommons.org/licenses/by-nc-nd/4.0/>).

**Correspondence:** Giuseppe Procino, Department of Biosciences, Biotechnologies and Biopharmaceutics, University of Bari, Via Orabona 4, Bari 70126, Italy. E-mail: [giuseppe.procino@uniba.it](mailto:giuseppe.procino@uniba.it)

<sup>7</sup>These authors equally contributed to this work.

Received 29 January 2016; revised 4 March 2016; accepted 10 March 2016

In the kidney, the antidiuretic hormone arginine vasopressin (AVP) is a critical regulator of water and electrolyte homeostasis. AVP is released from the pituitary gland into the bloodstream and binds to the type 2 vasopressin receptor (AVPR2),<sup>1</sup> a G protein-coupled receptor localized in the thick ascending limb of Henle, the distal convoluted tubule, and the collecting duct, acting mainly through the cAMP-protein kinase A pathway.

In the thick ascending limb of Henle, AVP stimulates NaCl reabsorption across the Na-K-Cl cotransporter (NKCC2), increasing its phosphorylation,<sup>2</sup> thus generating the corticomedullary osmotic gradient providing the driving force for water reabsorption in the kidney tubules.

In the CD, AVP stimulates the exocytosis of the water channel aquaporin 2 (AQP2)<sup>3</sup> at the apical membrane of the principal cells, dramatically increasing water reabsorption (for a review, see ref. 4). Inactivating mutations of the AVPR2 gene cause X-linked nephrogenic diabetes insipidus (XNDI), characterized by constant diuresis and the risk of severe dehydration.<sup>5</sup> Many studies have shown that hormones other than AVP also exhibit antidiuretic effect,<sup>6-10</sup> suggesting novel strategies to manage XNDI.

The  $\beta$ -adrenergic system controls several renal functions. In particular, types 1 and 2  $\beta$ -adrenoreceptors ( $\beta_{1-2}$ -AR)<sup>11</sup> regulate renal blood flow, glomerular filtration rate (GFR), sodium and water reabsorption, acid-base balance, and secretion of renin (for a review, see Johns *et al.*<sup>12</sup>).

Among  $\beta$ -ARs, the  $\beta_3$ -AR is the last identified member of this family. At first, it was shown to regulate lipolysis and thermogenesis in adipose tissue,<sup>13</sup> whereas subsequently it was shown to play important roles in the pathophysiology of the cardiovascular<sup>14</sup> and urinary<sup>15</sup> systems. However, its expression and possible physiologic role in the kidney remains to be fully clarified. There are indications in mice that  $\beta_3$ -AR mRNA is expressed by renal arteries.<sup>16</sup> In addition, in the rat kidney, a cDNA microarray screening showed that  $\beta_3$ -AR is expressed in the kidney medulla.<sup>17</sup> Moreover, in humans,  $\beta_3$ -AR polymorphisms seem to be associated with the effect of thiazide diuretics,<sup>16,18</sup> suggesting a role for  $\beta_3$ -AR in regulating renal water reabsorption. In this respect, demonstrating this novel role of  $\beta_3$ -AR in renal physiology is particularly intriguing in light of potential therapeutic applications of  $\beta_3$ -AR-acting drugs in diseases characterized by

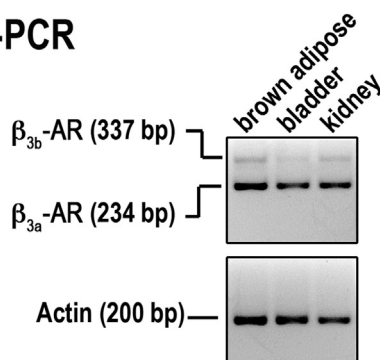
altered diuresis. Moreover,  $\beta_3$ -AR is relatively resistant to agonist-induced desensitization,<sup>19</sup> which would ensure prolonged pharmacologic stimulation *in vivo*. In addition, due to the limited number of tissues expressing  $\beta_3$ -AR, compared with  $\beta_{1-2}$ -AR,  $\beta_3$ -AR agonists are supposed to show a low systemic off-target effect.<sup>14</sup>

## RESULTS

### $\beta_3$ -AR expression in the mouse kidney

Reverse transcriptase polymerase chain reaction revealed that  $\beta_3$ -AR mRNA was clearly detectable in the RNA samples from the mouse kidney, brown adipose tissue, and bladder (Figure 1a). In particular, the intron-spanning primers amplified 2 bands of 234 bp and 337 bp, representing  $\beta_{3a}$ -AR and  $\beta_{3b}$ -AR transcripts, respectively.<sup>20</sup> Sequencing confirmed the specificity of the obtained bands (data not shown).

### a RT-PCR



### b Western blotting

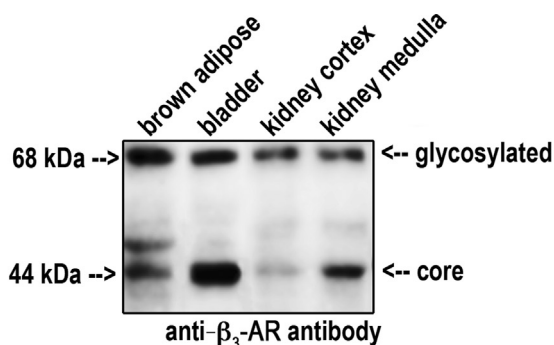


**Figure 1 | Expression of  $\beta_3$ -ARs mRNA and protein in mouse kidney.** (a) Total RNA from mouse kidney was probed for the presence of mRNA coding  $\beta_3$ -adrenergic receptors ( $\beta_3$ -ARs). Brown adipose tissue and bladder were used as positive controls. Two amplicons corresponding to  $\beta_{3b}$ -AR (337 bp) and  $\beta_{3a}$ -AR (234 bp) were visualized in all samples. Control reverse transcriptase polymerase chain reaction was performed using primers amplifying mouse  $\beta$ -actin. (b) Total protein extracts from mouse kidney cortex and total medulla were analyzed by Western blotting using anti- $\beta_3$ -AR antibodies. Two bands, corresponding to the core and the glycosylated protein, were detected in the kidney fractions at the same molecular size as those revealed in brown adipose and urinary bladder. Experiments were repeated 3 times with comparable results. RT-PCR, reverse transcriptase polymerase chain reaction.

Immunoblotting analysis revealed that mouse kidney cortex and total medulla expressed a band of 44 kDa for the core protein and 1 at 68 kDa for the glycosylated form in all samples (Figure 1b). Both bands were also revealed in  $\beta_3$ -AR-expressing control tissues.

### Immunolocalization of $\beta_3$ -ARs in the mouse kidney

As shown in Figure 2,  $\beta_3$ -AR was expressed at the apical and basolateral membrane of the epithelial cells of the thin ascending limb, identified by the presence of the kidney-specific chloride channel CIC-K1.<sup>21,22</sup>  $\beta_3$ -AR was also localized at the basolateral membrane of the epithelial cells of (i) the thick ascending limb of Henle, expressing the apical NKCC2 cotransporter<sup>23</sup>; (ii) the distal convolute tubule, expressing the apical thiazide-sensitive NaCl symporter (NCC)<sup>24</sup>; and (iii) the cortical CD and the outer medullary CD (the latter not shown), expressing AQP2 at the apical membrane.<sup>25</sup> The staining for  $\beta_3$ -AR completely disappeared when the anti- $\beta_3$ -AR antibody used for immunofluorescence was preadsorbed on its immunizing peptide (Supplementary Figure S1).

We also demonstrated that  $\beta_3$ -AR was neither expressed in the proximal convolute tubule nor in the thin descending limb of Henle's loop, the inner medullary CD, and the *vasa recta* (Supplementary Figure S2). Overall, the current data show that  $\beta_3$ -AR is localized in those nephron tracts also expressing AVPR2.

### Effect of $\beta_3$ -AR activation on cAMP production, AQP2 trafficking, and NKCC2 phosphorylation: *ex vivo* experiments

Our finding that  $\beta_3$ -AR is expressed in the AVPR2-positive kidney segments prompted us to investigate whether  $\beta_3$ -AR activation may mimic the effect of AVP on cAMP production, AQP2 intracellular trafficking, and NKCC2 activation. Using an *ex vivo* model consisting of freshly isolated mouse kidney tubule suspensions, we measured changes in intracellular cAMP concentrations in response to either the specific  $\beta_3$ -AR agonist BRL37344 (1, 10, 100  $\mu$ M) or the AVP analog 1-deamino-8-D-arginine-vasopressin (dDAVP),  $10^{-7}$  M, used as positive control for cAMP production (Figure 3a). Results are reported as the percentage of the cAMP concentration measured in resting tubules. Treatment with BRL37344 led to a concentration-dependent increase in intracellular cAMP levels, with the maximal effect observed at 10  $\mu$ M (+173%,  $P < 0.0001$ ).

Accordingly, we used 10  $\mu$ M BRL37344 for all the following experiments performed in freshly isolated live mouse kidney slices, untreated (resting) or incubated with either dDAVP or BRL37344 (Figure 3b). Confocal microscopy showed that both BRL37344 and dDAVP promoted AQP2 accumulation at the luminal plasma membrane of cortical collecting duct cells (Figure 3b, white arrows) compared with the cytoplasmic localization of AQP2 observed in control slices (Figure 3b, white arrowheads). In line with the absence of  $\beta_3$ -AR in the inner medullary CD, BRL37344 failed to induce AQP2 apical accumulation in this portion of the CD (not shown). Importantly, the effect of BRL37344 was prevented by

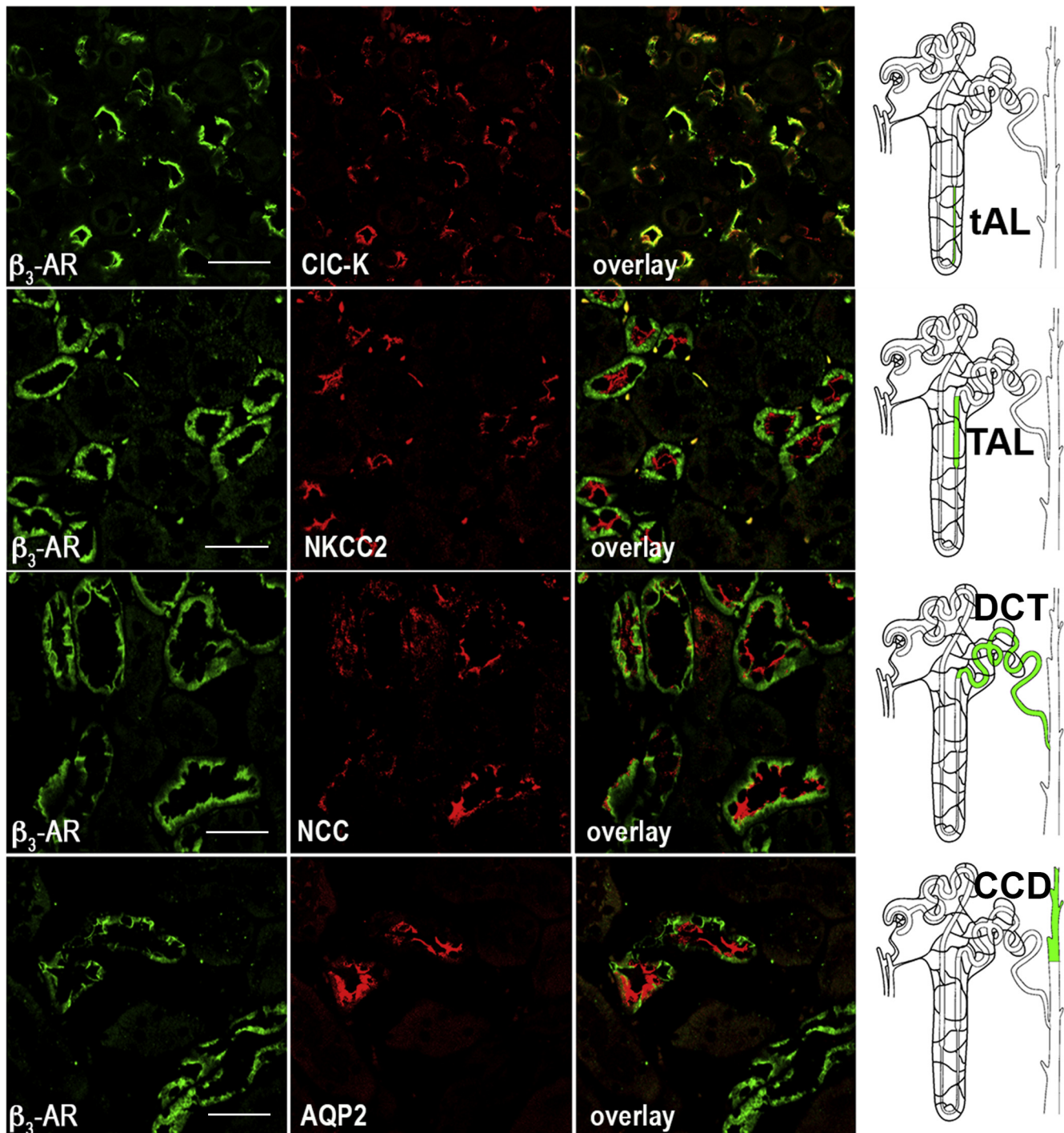


**Figure 2 | Immunolocalization of  $\beta_3$ -AR in mouse kidney.** Paraffin-embedded kidney sections (C57BL6/J, wild type) were immunostained with anti- $\beta_3$ -adrenergic receptor ( $\beta_3$ -AR) antibodies (green) and costained with antibodies against specific markers of different segments of the kidney tubule: kidney-specific chloride channel (CLC-K) channel for the thin ascending limb (tAL), Na-K-Cl cotransporter (NKCC2) for the thick ascending limb (TAL), NaCl symporter (NCC) for the distal convoluted tubule (DCT), and aquaporin 2 (AQP2) for the cortical collecting duct (CCD) (all in red). Overlay of the each double-staining experiment indicated significant expression of  $\beta_3$ -AR in the tAL, TAL, DCT, and CCD. Drawings of the nephron on the right show in light green the  $\beta_3$ -AR-positive segments. The same results were obtained in 5 different animals (bar = 20  $\mu$ m).

preincubation with either the  $\beta_3$ -AR-selective antagonist L748,337<sup>26</sup> or the protein kinase A inhibitor H89.<sup>27</sup>

Next, we evaluated the level of NKCC2 phosphorylation under the same experimental conditions using an antibody

against the regulatory phosphothreonine residues in the N-terminus of NKCC2.<sup>28</sup> Western blotting (Figure 3c and d) showed that p-NKCC2 increased by about 5-fold after BRL37344 treatment compared with resting conditions, an

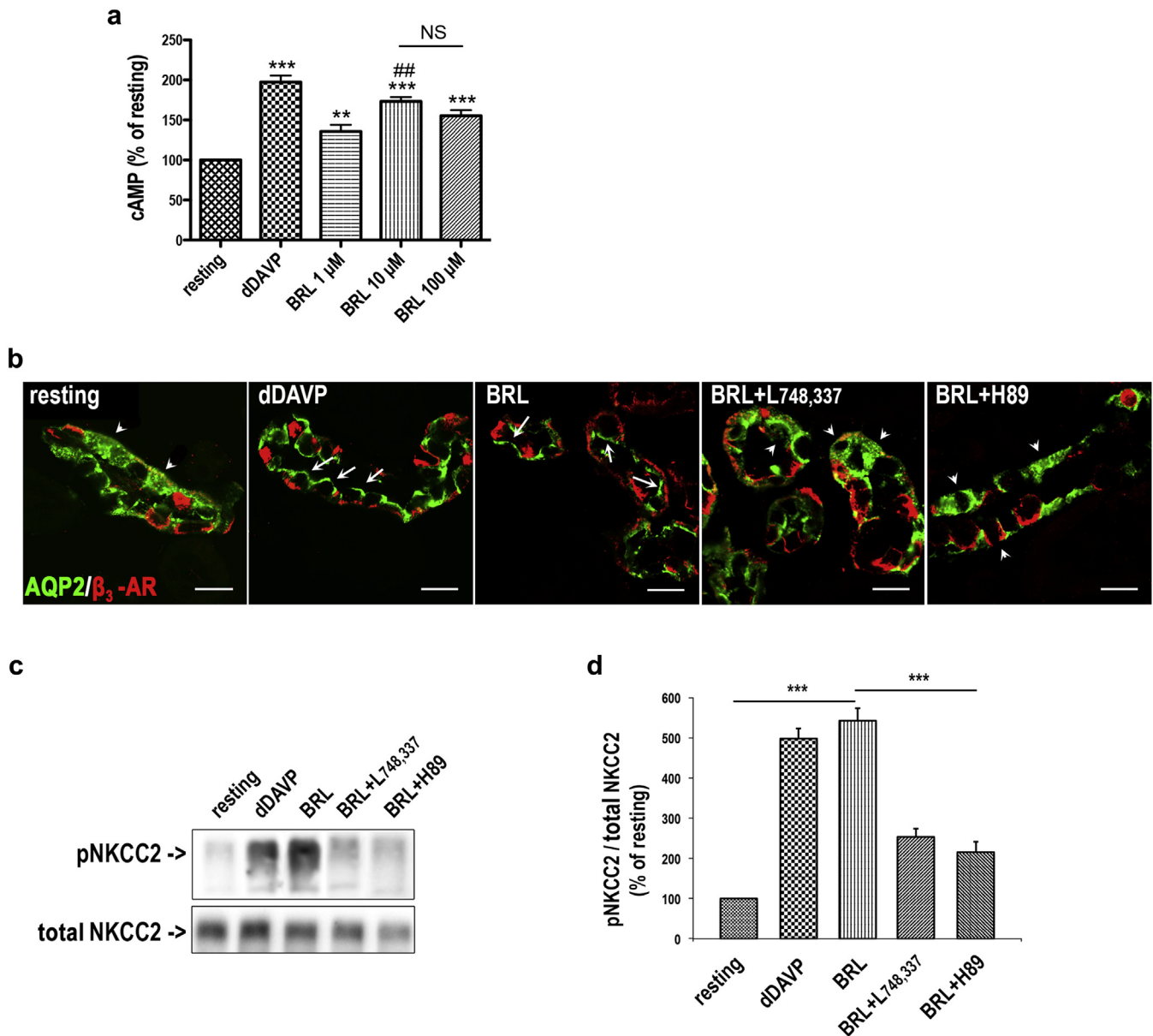


**Figure 3 | Ex vivo  $\beta_3$ -AR activation in a kidney tubule: intracellular cAMP measurements, AQP2 subcellular localization, and NKCC2 phosphorylation.** (a) 1-Deamino-8-D-arginine-vasopressin (dDAVP)- and BRL37344 (BRL)-induced cAMP production in mouse kidney tubule suspensions. Freshly isolated tubule suspensions from wild-type mice (12-week-old males, 3 per individual experiment) were pooled and equally distributed into 24-well plates. Samples were treated with dDAVP ( $10^{-7}$  M) or with the indicated concentrations of BRL for 60 minutes at  $37^\circ\text{C}$ . Total cAMP-generated in each well was normalized to the protein content. Three independent experiments were carried out. Data are expressed as the percentage of the cAMP content measured in resting cells  $\pm$  SEM. Significant differences between means were tested by 1-way analysis of variance with the Newman-Keuls posttest. Significance was accepted for  $P$  values  $< 0.05$ . \*\*\* $P < 0.0001$ , \*\* $P < 0.001$  compared with resting tubules. ### $P < 0.001$  compared with  $1\ \mu\text{M}$  BRL. (b) Freshly isolated kidney slices ( $250\ \mu\text{m}$ ) were rapidly cut after sacrifice, maintained in  $\text{CO}_2$ -equilibrated culture medium at  $37^\circ\text{C}$ , left untreated (resting), or incubated with dDAVP ( $10^{-7}$  M) or with BRL ( $10\ \mu\text{M}$  BRL). BRL was also incubated after preincubation with either the  $\beta_3$ -AR-antagonist (L748,337,  $10^{-7}$  M) or the protein kinase A inhibitor (H89) ( $10^{-5}$  M). Slices were treated as described and fixed, and ultrathin sections were stained for aquaporin 2 (AQP2) and  $\beta_3$ -adrenergic receptor ( $\beta_3$ -AR) and subjected to confocal microscopy. BRL was as effective as dDAVP in promoting AQP2 expression at the apical plasma membrane of cortical and outer medullary collecting duct cells (white arrows) compared with the intracellular localization of AQP2 observed in untreated samples (resting) or samples incubated with BRL after preincubation with L748,337 or H89 (white arrowheads) (bar =  $15\ \mu\text{m}$ ). (c) Kidney slices were treated as described, then lysed, and total protein extracts underwent Western blotting analysis using the anti-phosphorylated Na-K-Cl cotransporter (pNKCC2) and the anti-total NKCC2 antibodies. (d) Densitometric analysis showed a five-fold increase in pNKCC2 (normalized to total NKCC2) in samples treated with BRL or dDAVP, and the effect of BRL was significantly prevented by L748,337 and H89. Data are provided as mean  $\pm$  SEM and expressed as a percentage of the resting condition. Significant differences between means were tested by 1-way analysis of variance with the Newman-Keuls posttest. \*\*\* $P < 0.001$ . Comparable results were obtained in 3 different mice. NKCC2, Na-K-Cl cotransporter; NS, not significant.

effect comparable to that obtained with dDAVP. Pretreatment with either L748,337 or H89 significantly prevented this effect of BRL37344. Of note, incubation of kidney slices with either L748,337 or H89 alone did not change AQP2 subcellular localization or NKCC2 phosphorylation compared with resting slices (not shown).

To confirm that these effects of BRL37344 were ascribable to  $\beta_3$ -AR stimulation, we repeated these experiments on live kidney slices from  $\beta_3$ -AR-null mice ( $\beta_3$ -AR<sup>-/-</sup>).<sup>29</sup> Importantly, in the absence of  $\beta_3$ -AR functional expression, BRL37344 promoted neither AQP2 apical accumulation

(Figure 4a) nor NKCC2 phosphorylation (Figure 4b and c). In addition, in  $\beta_3$ -AR<sup>-/-</sup> mice, 10  $\mu$ M BRL37344 was unable to promote intracellular cAMP elevation in isolated kidney tubules (not shown).

#### Effect of $\beta_3$ -AR knockout on water and electrolyte handling in the mouse kidney

The effect of  $\beta_3$ -AR agonism on AQP2 and NKCC2, the major players involved in antidiuresis, prompted us to investigate whether  $\beta_3$ -AR inactivation may affect water and electrolyte handling in the kidney *in vivo*. To this end, we evaluated these

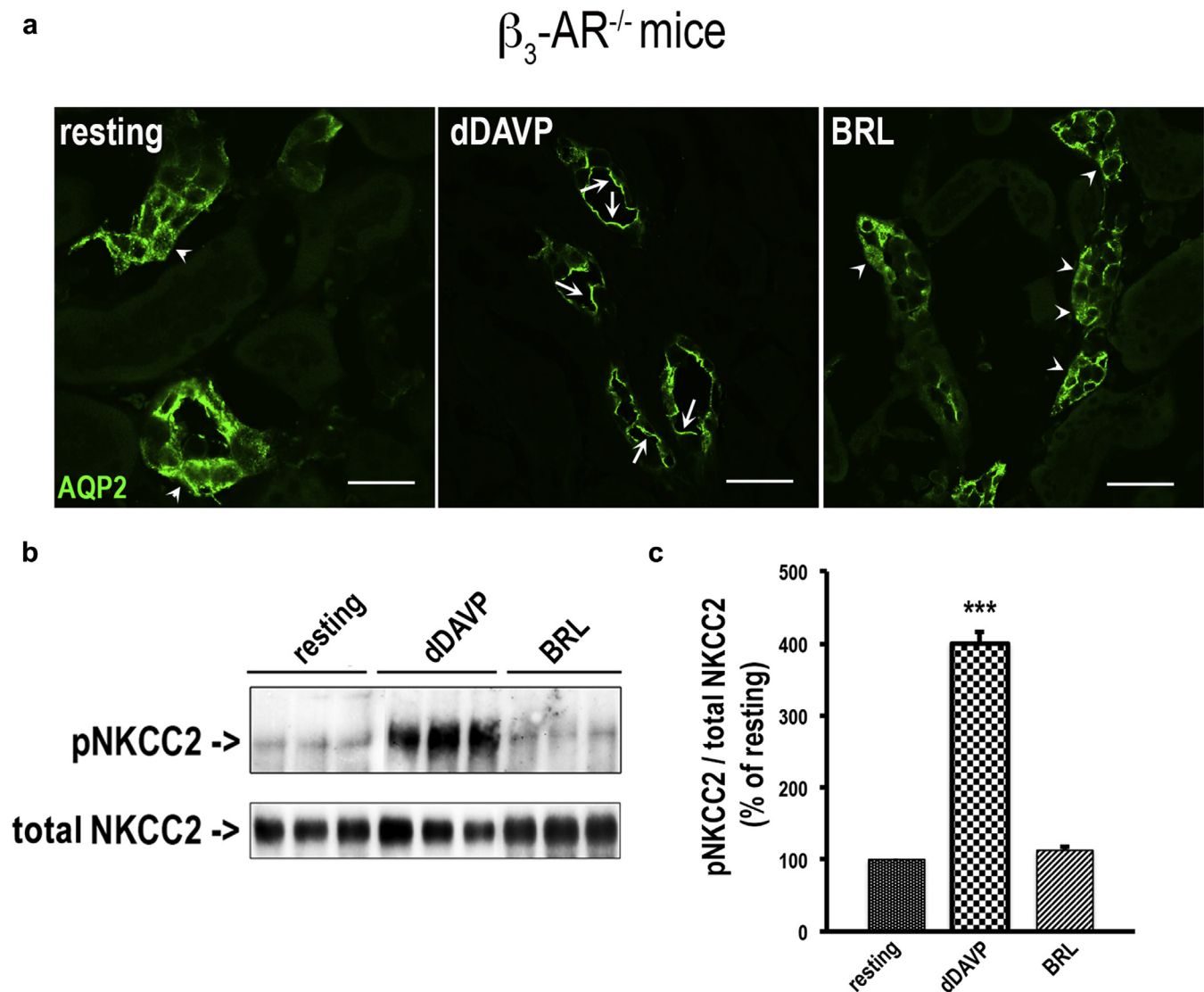


**Figure 4 | BRL37344 failed to induce AQP2 apical expression and NKCC2 phosphorylation in the kidney of  $\beta_3$ -AR-null mice.** (a) Freshly isolated kidney slices (250  $\mu$ m) were obtained from  $\beta_3$ -AR ( $\beta_3$ -adrenergic receptor) mice, maintained in CO<sub>2</sub>-equilibrated culture medium at 37 °C, and left untreated (resting) or incubated with desmopressin (dDAVP, 10<sup>-7</sup> M) or BRL37344 (BRL, 10  $\mu$ M). Slices were fixed, and ultrathin sections (5  $\mu$ m) were stained for AQP2 (aquaporin 2) and subjected to confocal laser-scanning microscopy. In  $\beta_3$ -AR mice, BRL was unable to promote AQP2 expression at the apical plasma membrane of cortical and outer medullary collecting duct cells. dDAVP was used as an internal control to promote AQP2 apical expression (bar = 10  $\mu$ m). Arrows indicate apical plasma membrane staining. Arrowheads indicate intracellular staining. (b) Slices were also lysed and protein extracts subjected to Western blotting analysis with antiphosphorylated Na-K-Cl cotransporter (pNKCC2) and total Na-K-Cl cotransporter (NKCC2) antibodies. (c) Densitometric analysis of pNKCC2, normalized to total NKCC2, showed that in  $\beta_3$ -AR mice, BRL was unable to increase NKCC2 phosphorylation compared with dDAVP. Data are provided as mean  $\pm$  SEM and expressed as the percentage of the resting condition. Significant differences between means were tested by 1-way analysis of variance with the Newman-Keuls posttest. \*\*\**P* < 0.0001. Comparable results were obtained in 3 different mice.

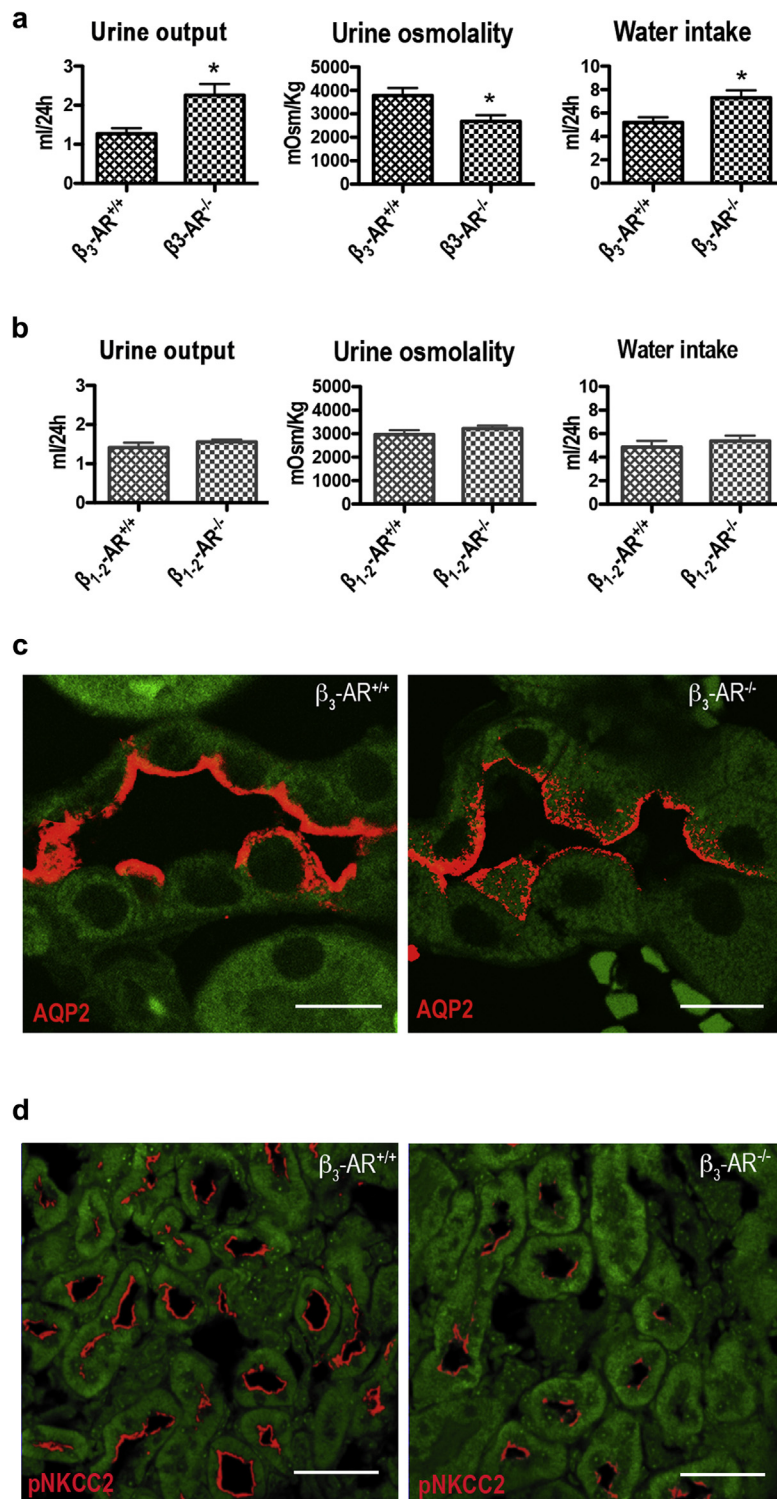


**Figure 5 | Mice lacking functional expression of  $\beta_3$ -AR showed mild polyuria and reduced urine osmolality.** (a)  $\beta_3$ -adrenergic receptor-null mice ( $\beta_3$ -AR<sup>-/-</sup>) and their age-matched controls ( $\beta_3$ -AR<sup>+/+</sup>) (8 in each group) were individually housed in metabolic cages for 5 days, and 24-hour urine output, urine osmolality, and water intake were measured daily. The analysis reports the mean  $\pm$  SEM values relative to 24-hour urine collection. In  $\beta_3$ -AR<sup>-/-</sup> mice, urine output was nearly 77% higher, urine osmolality 30% was lower, and water intake was 41% higher compared with control  $\beta_3$ -AR<sup>+/+</sup> mice. Statistical analysis was performed by unpaired *t* test. \**P* < 0.05. (b) The same experimental protocol was applied to  $\beta_{1,2}$ -AR-null mice ( $\beta_{1,2}$ -AR<sup>-/-</sup>) and their age-matched controls ( $\beta_{1,2}$ -AR<sup>+/+</sup>) (8 in each group). No statistically significant difference was observed in urine parameters and water intake between the 2 experimental groups. (c) Immunofluorescence analysis showed that  $\beta_3$ -AR<sup>-/-</sup> mice have reduced plasma membrane expression and higher subapical localization of AQP2 compared with control  $\beta_3$ -AR<sup>+/+</sup> mice (bar = 10  $\mu$ m). (d) Immunofluorescence analysis with the antiphosphorylated Na-K-Cl cotransporter (pNKCC2) showed also that  $\beta_3$ -AR<sup>-/-</sup> mice have reduced levels of activated NKCC2 (pNKCC2) (bar = 30  $\mu$ m). Comparable results were obtained in 3 different mice.

parameters in  $\beta_3$ -AR<sup>-/-</sup> mice<sup>29</sup> lacking  $\beta_3$ -AR functional expression and  $\beta_{1-2}$ -AR<sup>-/-</sup> knockout mice,<sup>30</sup> in which  $\beta_3$ -AR is the only expressed  $\beta$ -AR. Age-matched wild-type (wt) mice of each strain were used as controls ( $\beta_3$ -AR<sup>+/+</sup> and  $\beta_{1-2}$ -AR<sup>+/+</sup>). Strikingly, in  $\beta_3$ -AR<sup>-/-</sup>, diuresis was higher (by 77%), urine osmolality was lower (by 30%), and water intake was increased (by 40%) compared with  $\beta_3$ -AR<sup>+/+</sup> (Figure 5a). In contrast, urine parameters and water intake were comparable between  $\beta_{1-2}$ -AR<sup>+/+</sup> and  $\beta_{1-2}$ -AR<sup>-/-</sup> mice (Figure 5b). No significant differences in food intake were observed between mouse strains (not shown).

In line with these results, immunofluorescence analysis showed that, compared with control  $\beta_3$ -AR<sup>+/+</sup> mice,  $\beta_3$ -AR<sup>-/-</sup> mice have reduced AQP2 plasma membrane expression and increased subapical localization (Figure 5c).

Analysis of urine electrolytes, reported in Table 1, showed that  $\beta_3$ -AR<sup>-/-</sup> mice have significantly higher urine excretion of Na<sup>+</sup>, K<sup>+</sup>, and Cl<sup>-</sup> compared with their age-matched  $\beta_3$ -AR<sup>+/+</sup>. Instead, the plasma concentration of the same electrolytes and the GFR were comparable between  $\beta_3$ -AR<sup>-/-</sup> and  $\beta_3$ -AR<sup>+/+</sup> mice. These results suggest reduced activity of the NKCC2 transporter in  $\beta_3$ -AR<sup>-/-</sup> mice.

Immunofluorescence analysis showed that in  $\beta_3$ -AR<sup>-/-</sup> mice, the antibody against phosphorylated NKCC2 detected a lower amount of activated NKCC2 in the outer medulla compared with  $\beta_3$ -AR<sup>+/+</sup> mice (Figure 5d).

To further support this evidence, we analyzed the effects of bumetanide injection on natriuresis in both  $\beta_3$ -AR<sup>-/-</sup> and  $\beta_3$ -AR<sup>+/+</sup> mice (Supplementary Figure 3c and d). Natriuresis was higher in  $\beta_3$ -AR<sup>+/+</sup> than in  $\beta_3$ -AR<sup>-/-</sup> mice (355.4 ± 21.55% vs. 287 ± 27.5%; *P* < 0.0001), confirming that  $\beta_3$ -AR<sup>-/-</sup> mice have less basal NKCC2 cotransporter activity to inhibit.

Of note, the maximal urine concentrating ability of  $\beta_3$ -AR<sup>-/-</sup> mice on a water deprivation test was comparable to that of  $\beta_3$ -AR<sup>+/+</sup> mice (Supplementary Figure S3a and b).

### Effect of $\beta_3$ -AR stimulation on urine output

Next, to uncover the possible antidiuretic effect of pharmacologic stimulation of  $\beta_3$ -AR in mice, we examined whether

**Table 1 | Plasma electrolyte concentrations, renal 24-h electrolyte excretion, GFRs, and food intake in  $\beta_3$ -AR<sup>+/+</sup> and  $\beta_3$ -AR<sup>-/-</sup> mice**

	Electrolytes	$\beta_3$ -AR <sup>+/+</sup>	$\beta_3$ -AR <sup>-/-</sup>	<i>P</i> Value
Plasma	Na <sup>+</sup> (mEq/l)	139.0 ± 5.57	141.3 ± 0.67	NS
	K <sup>+</sup> (mEq/l)	6.73 ± 0.29	6.43 ± 0.19	NS
	Cl <sup>-</sup> (mEq/l)	108.0 ± 3.22	106.3 ± 2.67	NS
	Ca <sup>2+</sup> (mEq/l)	3.16 ± 0.53	3.34 ± 0.44	NS
Urine	Na <sup>+</sup> (mEq/24 hr)	0.19 ± 0.02	0.27 ± 0.01	<i>P</i> < 0.01
	K <sup>+</sup> (mEq/24 hr)	0.18 ± 0.02	0.23 ± 0.01	<i>P</i> < 0.05
	Cl <sup>-</sup> (mEq/24 hr)	0.45 ± 0.04	0.59 ± 0.03	<i>P</i> < 0.01
	Ca <sup>2+</sup> (mEq/24 hr)	0.005 ± 0.0006	0.005 ± 0.0005	NS
	GFR (μl/min)	235.5 ± 20.76	253.8 ± 30.94	NS
	Food intake (g)	5.07 ± 0.08	5.14 ± 0.08	NS

Values are means ± SEM of measurements in 8 mice/genotype. Statistical analysis was performed using an unpaired *t* test.

GFR, glomerular filtration rate; NS, not significant.

BRL37344 could *per se* induce antidiuresis.  $\beta_3$ -AR<sup>+/+</sup> and  $\beta_3$ -AR<sup>-/-</sup> mice received a single i.p. injection of BRL37344 (0.6 mg/kg) or phosphate-buffered saline (PBS) alone (vehicle). Urine samples were collected for 4 hours after injections, the first time point at which all BRL37344-treated animals began to urinate. Diuresis, urine osmolality, and urine electrolyte excretion were analyzed and are shown in Figure 6. Notwithstanding the differing diuresis in  $\beta_3$ -AR<sup>-/-</sup> and  $\beta_3$ -AR<sup>+/+</sup> mice, we expressed our results as a percentage of the values measured in vehicle-treated animals of each genotype. Strikingly, BRL37344 greatly reduced the diuresis in  $\beta_3$ -AR<sup>+/+</sup> mice but not in  $\beta_3$ -AR<sup>-/-</sup> mice (Figure 6a). Concomitantly, BRL37344 significantly increased urine osmolality only in  $\beta_3$ -AR<sup>+/+</sup> mice (Figure 6b). Interestingly, in  $\beta_3$ -AR<sup>+/+</sup> mice, urine excretion of Na<sup>+</sup>, K<sup>+</sup>, and Cl<sup>-</sup>, normalized to the volume of diuresis, were significantly reduced by BRL37344 (Figure 6c–e). Of note, the GFR in  $\beta_3$ -AR<sup>+/+</sup> mice, measured at 1, 2, 3, and 4 hours after BRL37344 treatment, was not affected (Figure 6f).

### Effect of $\beta_3$ -AR stimulation on diuresis of mice lacking AVPR2

Next, we investigated whether the potent antidiuretic effect of BRL37344 observed in  $\beta_3$ -AR<sup>+/+</sup> mice could bypass the inactivation of the AVP signaling in mice lacking AVPR2.<sup>12,31</sup> Mice received a single i.p. injection of BRL37344 (0.6 mg/kg) or PBS alone (vehicle). Urine samples were collected every hour for 3 hours, and diuresis (Figure 7a) and urine osmolality (Figure 7b) were reported. Strikingly, 1 hour after the injection, the urine output of all BRL37344-treated mice was reduced to zero compared with vehicle-treated mice (Figure 7a, 1 hour). Therefore, we could not measure urine osmolality at this time point (Figure 7b, 1 hour). Two hours after injection, the diuresis of BRL37344-treated mice was still dramatically reduced compared with vehicle-treated animals (Figure 7a, 2 hours) and urine osmolality increased (Figure 7b, 2 hours). Three hours postinjection, the effect BRL37344 on diuresis still persisted (Figure 7a, 3 hours), whereas that on urine osmolality partially reversed (Figure 7b, 3 hours).

### DISCUSSION

The possible expression and physiologic role of  $\beta_3$ -AR in the kidney has not been investigated in depth thus far. The present results show  $\beta_3$ -AR expression in the same AVPR2-expressing tubules. Because it is known that, similar to AVPR2,  $\beta_3$ -AR activates the cAMP pathway,<sup>32</sup> we hypothesized that pharmacologic stimulation of  $\beta_3$ -AR might regulate the trafficking/activity of AQP2 and NKCC2 involved in the AVP-elicited antidiuresis in the kidney.<sup>2,3</sup> We first demonstrated that BRL37344 significantly increases cAMP production and promotes both AQP2 apical accumulation and NKCC2 phosphorylation/activation, suggesting that, similar to AVP,  $\beta_3$ -AR agonists may increase reabsorption of water and solutes in the kidney.

The pharmacologic profile of BRL37344 indicates that it may have an intrinsic activity at  $\beta_1$ -ARs or  $\beta_2$ -ARs.<sup>33</sup> As shown by the current results, BRL37344 effects on AQP2 and

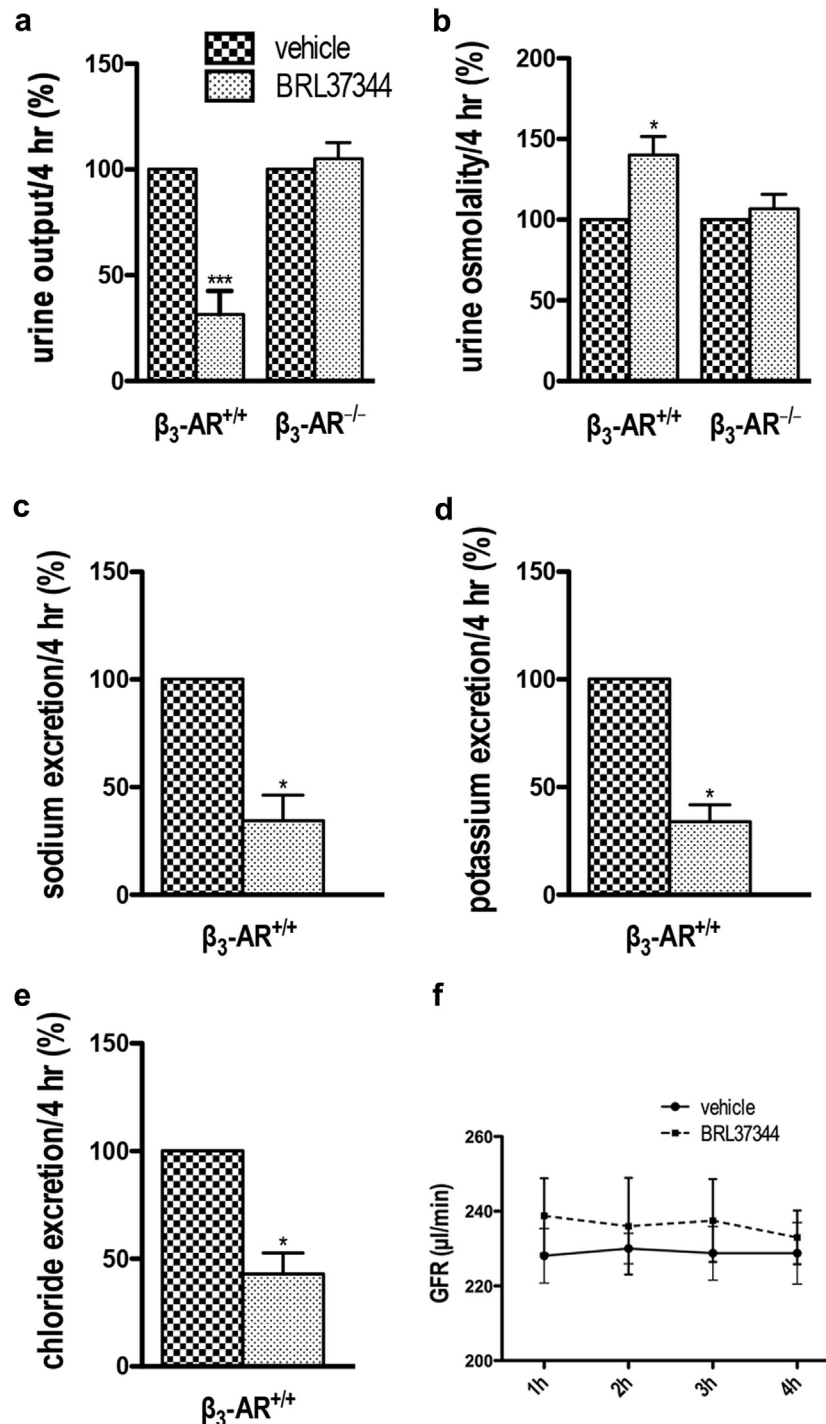


**Figure 6 | Effect of  $\beta_3$ -AR stimulation on urine concentrating ability in  $\beta_3$ -AR<sup>+/+</sup> mice.**  $\beta_3$ -adrenergic receptor ( $\beta_3$ -AR)-null ( $\beta_3$ -AR<sup>-/-</sup>) mice and their age-matched controls ( $\beta_3$ -AR<sup>+/+</sup>) (10 of each genotype) were individually acclimatized in metabolic cages for 48 hours; 5 received a single i.p. injection of BRL37344 (BRL) (0.6 mg/kg), whereas 5 control animals received phosphate-buffered saline alone (vehicle). Urine samples were collected for 4 hours after injection. Urine output (**a**) and urine osmolality (**b**) were measured in  $\beta_3$ -AR<sup>+/+</sup> and  $\beta_3$ -AR<sup>-/-</sup> mice and expressed as a percentage of control values measured in vehicle-injected animals  $\pm$  SEM. Urine output of  $\beta_3$ -AR<sup>+/+</sup> mice decreased  $\sim$ 70% and urine osmolality increased  $\sim$ 40% after BRL37344 (BRL) injection. No significant effect was seen in  $\beta_3$ -AR<sup>-/-</sup> mice. Significant differences between means were tested by 1-way analysis of variance with the Newman-Keuls posttest. \* $P < 0.05$ , \*\*\* $P < 0.0001$ . (**c,d,e**) Urine excretion of Na<sup>+</sup>, K<sup>+</sup>, and Cl<sup>-</sup>, normalized for the urine volume, measured in  $\beta_3$ -AR<sup>+/+</sup> mice. Data are reported as a percentage of the values measured in vehicle-injected mice  $\pm$  SEM. Significant differences between means were tested by the Mann-Whitney  $U$  test. \* $P < 0.05$ . (**f**) Glomerular filtration rate (GFR) of  $\beta_3$ -AR<sup>+/+</sup> conscious mice was measured at 1, 2, 3, and 4 hours after injection of BRL or vehicle alone. No significant difference was found at each time point between BRL- and vehicle-injected mice. Significant differences between means were tested by 2-way analysis of variance with a Bonferroni posttest.

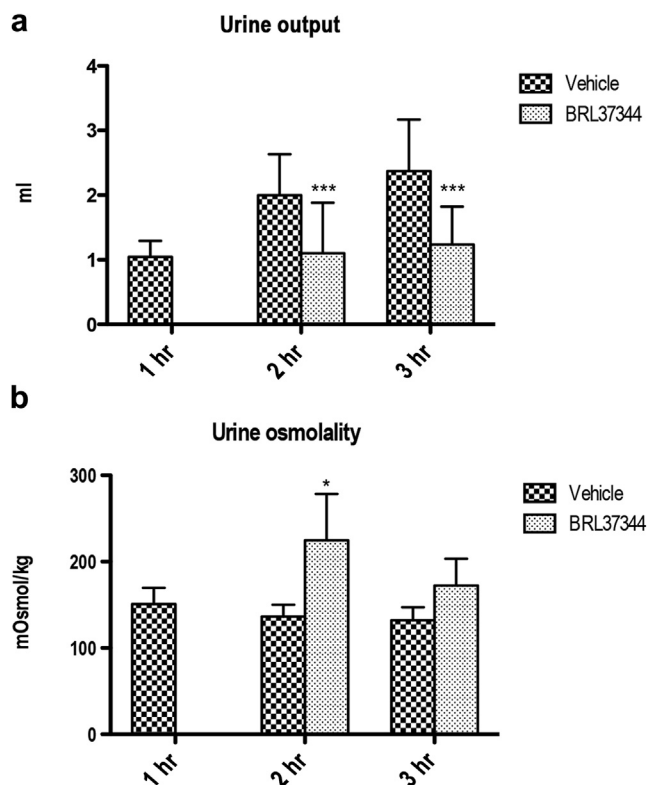


**Figure 7 |  $\beta_3$ -Adrenergic receptor stimulation promotes antidiuresis in mice lacking functional expression of the arginine vasopressin receptor type 2.** Ten  $V2R^{fl/y}Esr1-Cre$  mice were acclimatized in mouse metabolic cages for 48 hours; 5 received a single i.p. injection of BRL37344 (0.6 mg/kg), whereas 5 control mice received phosphate-buffered saline alone (vehicle). Urine samples were collected every hour for 3 hours from both groups, and urine output (a) and urine osmolality (b) at each time point were reported. One hour after the injection, the urine output of BRL37344-treated mice was reduced to zero compared with vehicle-injected animals (vehicle) (diuresis, 1 hour). Two hours after injection, urine output of treated mice was still dramatically reduced compared with control animals (diuresis, 2 hours). Urine osmolality increased in BRL37344-injected animals (urine osmolality, 2 hours). At 3 hours postinjection, the effect of BRL on the urine output still persisted (urine output, 3 hours), whereas the effect on urine osmolality partially reversed (urine osmolality, 3 hours). The analysis reports the mean  $\pm$  SEM values. Significant differences between measurements were tested by 2-way analysis of variance with a Bonferroni posttest for diuresis and by 1-way analysis of variance with a Bonferroni posttest. \* $P < 0.05$ ; \*\*\* $P < 0.001$ .

NKCC2 are prevented by the  $\beta_3$ -AR antagonist L748,337 and are not observed in  $\beta_3$ -AR $^{-/-}$  mice, thus supporting the notion that BRL37344 acts selectively at  $\beta_3$ -AR at the dose used and excluding an off-target effect.

Here we also show that  $\beta_3$ -AR $^{-/-}$  mice are characterized by mild polyuria, lower urine osmolality, and increased urinary excretion of  $\text{Na}^+$ ,  $\text{K}^+$ , and  $\text{Cl}^-$  but not  $\text{Ca}^{++}$ . Increased water excretion is in line with the observed reduced plasma membrane expression of AQP2 in the cortical collecting duct of  $\beta_3$ -AR $^{-/-}$ . In addition, increased  $\text{Na}^+$ ,  $\text{K}^+$ , and  $\text{Cl}^-$  excretion in  $\beta_3$ -AR $^{-/-}$  is in line with decreased NKCC2 activity, as also supported by the findings that  $\beta_3$ -AR $^{-/-}$  mice show less activated NKCC2 at the plasma membrane and a less pronounced natriuretic response to bumetanide.

The fact that food consumption in  $\beta_3$ -AR $^{-/-}$  mice is comparable to that of  $\beta_3$ -AR $^{+/+}$  mice (Table 1) seems to exclude that solute diuresis can explain the polyuria of  $\beta_3$ -AR $^{-/-}$  mice. Neither defect of AVP release (central polydipsia) can explain the polyuria of  $\beta_3$ -AR $^{-/-}$  mice because these mice show normal urine-concentrating abilities under a water deprivation challenge.

We also show that  $\beta_3$ -AR $^{-/-}$  mice have normal plasma levels of  $\text{Na}^+$ ,  $\text{K}^+$ ,  $\text{Cl}^-$ , and  $\text{Ca}^{++}$  indicating that their polyuric phenotype is neither induced by hypercalciuria/hypercalcemia nor by hypokalemia.<sup>34–36</sup> In addition, the polyuria in  $\beta_3$ -AR $^{-/-}$  mice is not a consequence of an increased GFR, which is comparable to that in  $\beta_3$ -AR $^{+/+}$  mice. On the other hand,  $\beta_{1-2}$ -AR $^{-/-}$  do not show alterations of urine output and osmolality, suggesting that  $\beta_3$ -AR, rather  $\beta_1$ -AR and  $\beta_2$ -AR, regulate these urine parameters. However, the question whether  $\beta_3$ -AR is more important than  $\beta_1$ -AR and  $\beta_2$ -AR in baseline renal function cannot be solved by the current study as we cannot compare the urine-concentrating ability of  $\beta_3$ -AR $^{-/-}$  and  $\beta_{1-2}$ -AR $^{-/-}$  mice. The 2 strains result from a different genetic background, and early studies showed that renal parameters significantly differ in mice of different strains.<sup>37</sup>

In line with the stimulatory effect of  $\beta_3$ -AR activation on AQP2 subcellular localization and NKCC2 phosphorylation, BRL37344 exerts a potent antidiuretic effect in  $\beta_3$ -AR $^{+/+}$  mice but not in  $\beta_3$ -AR $^{-/-}$  mice, thus confirming our *ex vivo* data on its specific action at the  $\beta_3$ -AR. The additional finding that in  $\beta_3$ -AR $^{+/+}$  mice, BRL37344 reduces urinary excretion of  $\text{Na}^+$ ,  $\text{K}^+$ , and  $\text{Cl}^-$  but not  $\text{Ca}^{++}$  and induces a 70% reduction of the urine output, whereas urine osmolality is increased by  $\sim 40\%$  may be explained by assuming that  $\beta_3$ -AR stimulation promotes not only water but also salt reabsorption in the kidney. In line with this possibility, the strong reduction of urine output observed in BRL37344-treated mice is independent of the decrease in the GFR.

$\beta_3$ -ARs are also expressed in the hypothalamus<sup>38</sup>; thus, the possibility exists that the antidiuretic effect of BRL37344 may involve hypothalamic regulation of AVP release. Our results in AVPR2-null mice<sup>31</sup> seem to exclude this possibility. In these mice, the classic symptoms of XNDI develop.<sup>39–41</sup> As shown here, a single i.p. injection of BRL37344 greatly reduces the diuresis and increases urine osmolality, supporting the notion that, *in vivo*,  $\beta_3$ -AR agonism triggers AVP-independent antidiuresis. In addition, results in live kidney slices, demonstrating that BRL37344 induces cAMP production, AQP2 plasma membrane accumulation, and NKCC2 phosphorylation/activation in the thick ascending limb of Henle, provide additional, although indirect, evidence that BRL37344 triggers its effect independently of central  $\beta_3$ -AR activation.

The current results cannot exclude that the effects of BRL37344 on urine output may be related to the systemic effects of the drug on arterial pressure. However, it has been shown in rats that BRL37344 reduces arterial pressure by  $\sim 14\%$ <sup>42</sup>; therefore, it is unlikely that such an effect may be responsible for the observed 70% reduction in urine output.

In conclusion, our experimental data indicate that (i) in mice,  $\beta_3$ -ARs are expressed in most of the AVP-sensitive nephron segments; (ii)  $\beta_3$ -AR stimulation promotes AQP2 plasma membrane accumulation and NKCC2 activation, thus increasing water and salt reabsorption in the kidney tubule; (iii) this effect is likely mediated by an increase of intracellular cAMP; and (iv)  $\beta_3$ -AR agonism induces antidiuresis in mice lacking AVPR2.

Taken together, these data suggest an unexplored role of sympathetic stimulation via the  $\beta_3$ -AR in promoting antidiuresis under physiologic conditions. Some evidence indicates that there is a synaptic contact between renal sympathetic varicosities and renal tubular epithelial cell basolateral membranes.<sup>12,43</sup> In this respect, the current data support the hypothesis that sympathetic stimulation of  $\beta_3$ -ARs, upregulating NKCC2 and AQP2 activity, can enhance solutes and water reabsorption in the nephron, thus eliciting an antidiuretic effect. Although we restricted our investigation to the regulatory role of  $\beta_3$ -ARs on AQP2 and NKCC2, the possible effect of  $\beta_3$ -AR stimulation on other Na/Cl transporters or additional AQPs, participating in the countercurrent multiplier system, is worth further investigation.

The observation that  $\beta_3$ -AR<sup>-/-</sup> mice are polyuric but show normal urine-concentrating ability during water deprivation suggest that, under physiologic conditions,  $\beta_3$ -AR activation by sympathetic nerves does not provide an additional mechanism, corroborating the kidney antidiuretic response to AVP. Although much work remains to be done to fully understand the role of  $\beta_3$ -ARs in water and salt reabsorption during sympathetic activation, the current results are potentially relevant for the development of novel pharmacologic approaches to the treatment of diseases caused by AVPR2-altered signaling, including XNDI, polycystic kidney diseases, and the syndrome of inappropriate secretion of AVP. For instance, in XNDI patients,  $\beta_3$ -AR agonists may bypass the lack of AVPR2 function, restore NKCC2 and AQP2 activity, and improve the unpaired urine concentration mechanism. It must be emphasized that patients with autosomal forms of NDI<sup>40</sup> due to mutations of the AQP2 gene would not benefit from this potential treatment.

Further studies are needed to verify this proof-of-concept, but the ameliorative effect of BRL37344 on renal concentrating abilities of AVPR2-null mice strongly encourages studies in this direction. In particular, we suggest that agonists of the human  $\beta_3$ -AR, such as mirabegron,<sup>44</sup> already used to treat an overactive bladder, may either improve the impaired concentrating ability of the kidney or increase the beneficial effects of the current XNDI therapy.

## MATERIALS AND METHODS

### Antibodies and reagents

Polyclonal antibodies against  $\beta_3$ -AR (cat. nos. sc-50436 and sc-1473) were obtained from Santa Cruz Biotechnology (Dallas, TX) and were previously validated for Western blotting and immunofluorescence analysis.<sup>45,46</sup> Antibodies against AQP1 (cat. no. sc-20810), and CD-31 (cat. no. sc-1506), BRL37344 (cat. no. sc-200154), L748,337 (cat. no.

sc-204044) were from Santa Cruz Biotechnology. H-89 (cat. no. B1427), and [deamino-Cys<sup>1</sup>, D-Arg<sup>8</sup>]-vasopressin (dDAVP, cat. no. V-1005) were from Sigma (St. Louis, MO). Antibody anti-CLC-K (cat. no. ACL-004) was from Alomone Labs (Jerusalem, Israel). Antibodies anti-NKCC2 (cat. no. AB3562P) were from Merck Millipore (Billerica, MA). Antibodies anti-NCC (cat. no. SPC-402D) were from StressMarq Biosciences Inc. (Victoria, BC, Canada). The antibody against human AQP2 was previously described.<sup>47</sup> The antibody against the phosphorylated threonines 96 and 101 of phosphorylated mouse NKCC2<sup>28</sup> was kindly provided by Prof. Biff Forbush, Yale University.

### $\beta_3$ -AR pharmacology

BRL37344 is a well-known  $\beta_3$ -AR agonist<sup>48</sup> that has been previously used in mice.<sup>49–51</sup> BRL37344 displays a rank order of potency at the human  $\beta$ -ARs, i.e.,  $\beta_3$ -AR >  $\beta_2$ -AR >  $\beta_1$ -AR, with an approximately 20-fold and 100-fold higher selectivity for  $\beta_3$ -AR versus  $\beta_2$ -AR and  $\beta_1$ -AR, respectively.<sup>52</sup> BRL37344 has been found to be effective at 10  $\mu$ M in the human isolated internal anal sphincter model,<sup>53</sup> in human retinal endothelial cells,<sup>54</sup> and in mouse retinal explants.<sup>55</sup>

L748,337 has been reported as one of the very few antagonists with a high selectivity for  $\beta_3$ -AR.<sup>56</sup> Nonetheless, L748,337 remains the most suitable  $\beta_3$ -AR antagonist currently available.<sup>26</sup>

### RNA isolation and reverse transcriptase polymerase chain reaction

Total RNA was extracted from mouse brown adipose tissue, the bladder, and the kidney by the TRIzol reagent and reverse-transcribed into cDNA using SuperScript VILO cDNA Synthesis Kit (Thermo Fisher Scientific, Waltham, MA).

The mouse  $\beta_3$ -AR intron-spanning primers were previously reported.<sup>20</sup> As a positive control, mouse  $\beta$ -actin cDNA was amplified using specific primers. Polymerase chain reaction was performed using Taq DNA polymerase recombinant (Life Technologies, Carlsbad, CA) according to the following: (94°C, 3 minutes)  $\times$  1 cycle and (94°C, 45 seconds; 55°C, 30 seconds; 72°C, 1 minute)  $\times$  40 cycles. Amplified products were analyzed on 3% agarose gel. Sequencing was performed by BMR Genomics (Padova, Italy), using the method of Sanger.

### Cell and tissue fractionation and immunoblotting

Brown adipose tissue, bladder, and kidney cortex/total medulla were isolated from male C57BL/6J mice and homogenized in radioimmunoprecipitation assay buffer.<sup>57</sup> Where reported, kidney slices were lysed in antiphosphatase buffer.<sup>2</sup>

Fifteen micrograms of each lysate were separated by sodium dodecylsulfate-polyacrylamide gel electrophoresis and analyzed by Western blotting. After blocking with 3% bovine serum albumin, blots were incubated with anti- $\beta_3$ -AR antibody (sc-50436, 1:200) and anti-p-NKCC2 antibodies (1:1000) followed by horseradish peroxidase-conjugated secondary antibody.

Blots were revealed by enhanced chemiluminescence, with Chemidoc XRS, equipped with Image Lab Software (Bio-Rad, Hercules, CA) and quantified with ImageJ software.

### Immunofluorescence

Mouse kidneys were fixed with 4% paraformaldehyde in PBS at 4°C, dehydrated in graded ethanol, and embedded in paraffin wax. Serial sections, 5  $\mu$ m thick, were deparaffinized, rehydrated, and subjected to immunofluorescence analysis. Antigen retrieval was performed by boiling sections in citrate buffer (10 mM sodium citrate, pH 6). After blocking with 1% bovine serum albumin in PBS for 30 minutes,

sections were incubated with the primary antibodies  $\beta_3$ -AR (sc-1473), AQP2, AQP1, CLC-K, NKCC2, CD31, NCC, and phosphorylated NKCC2.

Sections were incubated with AlexaFluor-conjugated secondary antibodies (Life Technologies). Confocal images were obtained with a confocal microscope (TSC-SP2, Leica; Wetzlar, Germany).

### Preparation of kidney tubule suspensions and cAMP assay

Kidneys from FVB/C57/129/DBA mice (10-week old males) were minced and enzymatically digested as previously reported.<sup>10</sup> Aliquots of tubule suspensions were preincubated with the phosphodiesterase inhibitor IBMX for 10 minutes at 37°C. Subsequently, BRL37344 (1, 10, and 100  $\mu$ M) or dDAVP (100 nM) were added, and reactions were carried out for 45 minutes at 37°C. Total intracellular cAMP was determined by enzyme-linked immunosorbent assay, as previously reported.<sup>10</sup>

### Kidney tissue slices: preparation and treatment

C57BL/6J male mice were anesthetized with tribromoethanol (250 mg/kg) and euthanized by cervical dislocation. Kidneys were excised, and thin transversal slices (250  $\mu$ m) were cut using a McIlwain Tissue Chopper (Ted Pella Inc.; Redding, CA, United States). Slices were left at 37°C for 15 minutes in Dulbecco's Modified Eagle Medium/F12 medium pre-equilibrated with 5% CO<sub>2</sub>, then stimulated for 40 minutes with dDAVP (10<sup>-7</sup> M) or BRL37344 (10<sup>-5</sup> M), the latter alone or after 30 minutes of preincubation with either L748,337 (10<sup>-7</sup> M) or H89 (10<sup>-5</sup> M). Slices were either processed for immunoblotting analysis or fixed in 4% paraformaldehyde and processed for immunofluorescence as described previously.

### Animal studies

All animal experiments were approved by the Institutional Committee on Research Animal Care, in accordance with the Italian Institute of Health Guide for the Care and Use of Laboratory Animals. Mice were maintained on a 12-hour light/12-hour dark cycle, with free access to water and food.

$\beta_3$ -AR<sup>-/-</sup> and  $\beta_3$ -AR<sup>+/+</sup> mice<sup>58</sup> were purchased from Jackson Laboratory (Bar Harbor, ME, United States).  $\beta_{1-2}$ -AR<sup>-/-</sup> and  $\beta_{1-2}$ -AR<sup>+/+</sup> mice<sup>30</sup> were generated as previously described.<sup>59,60</sup> Metabolic cages were used to measure urine output, osmolality, and water intake. Mice received a single i.p. injection of BRL37344 (0.6 mg/kg) or PBS alone. Electrolytes were measured using the ion selective electrode method.

The GFR of conscious mice was measured as previously reported.<sup>61</sup> AVPR2 knockout mice (V2R<sup>fl/fl</sup> and V2R<sup>fl/y</sup> Esr1-Cre mice) were previously described.<sup>31</sup>

V2R<sup>fl/y</sup> Esr1-Cre mice received a single i.p. injection of BRL37344 (0.6 mg/kg) or PBS alone and urine output and osmolality were monitored every hour for 3 hours. Urine osmolality was measured using a vapor pressure osmometer.

### Statistical analysis

For statistical analysis, GraphPad Prism software (La Jolla, CA) was used. The statistical analysis performed is indicated in the figure legends.

### DISCLOSURE

All the authors declared no competing interests.

### ACKNOWLEDGMENTS

This work was funded by grants GGP12040 and GGP15083 from the Fondazione Telethon to MS, from grant MRAR08P011 from the

Agenzia Italiana del Farmaco (AIFA) to MS, and grant RF02351158 from the Ministero della Salute to PB. We are grateful to J. H. Wess, National Institute of Diabetes and Digestive and Kidney Diseases, for providing the V2R<sup>fl/y</sup> and V2R<sup>fl/fl</sup> mice. The antibody against the phosphorylated threonines 96 and 101 of mouse NKCC2 (p-NKCC2) was kindly provided by Prof. B. Forbush, Yale University. We are also grateful to Silvia Torretta, Gaetano De Vito, Maurizio Cammalleri, Filippo Locri, Vincenzo Calderone, Alma Martelli, and Dominga Lapi for technical assistance with the animal experiments and maintenance of transgenic mouse colonies.

### SUPPLEMENTARY MATERIAL

**Figure S1.** Pre-adsorption of anti  $\beta_3$ -AR antibody on its immunizing peptide completely abolished the immunostaining of  $\beta_3$ -AR in mouse kidney sections. Goat anti $\beta_3$ -AR (#SC1473) was preadsorbed on its immunizing peptide (SC1473p) and used to immunostain paraffin-embedded mouse kidney sections. Compared to whole antibody, immunodepleted antibody failed to detect  $\beta_3$ -AR-positive tubule in both kidney cortex and medulla (bar = 50  $\mu$ m).

**Figure S2.** Immunolocalization of  $\beta_3$ -AR in mouse kidney. Paraffin-embedded kidney sections (C57BL6/J, wt) were immunostained with anti  $\beta_3$ -AR antibodies (green) and co-stained with antibodies against specific markers of different segments of the kidney tubule or vasculature: AQP1 for the proximal tubule (PT) and the thin descending limb (TDL), AQP2 for the inner medullary collecting duct (IMCD) and CD31 for the endothelium of *Vasa Recta* (all in red). Overlay of the each double staining experiment indicated that  $\beta_3$ -AR was neither expressed in the PT nor in the TDL nor in the IMCD nor in the *Vasa Recta*. Drawings of the nephron on the right column indicated in red the  $\beta_3$ -AR-negative tubule or vascular portions.  $\beta_3$ -AR was expressed at the basolateral plasma membrane in all the tubules where it is expressed. Same results were obtained in at least 5 animals (bar = 20  $\mu$ m).

**Figure S3.** Water deprivation test and bumetanide-induced diuresis and natriuresis.  $\beta_3$ -AR-null mice ( $\beta_3$ -AR<sup>-/-</sup>) and their age-matched controls ( $\beta_3$ -AR<sup>+/+</sup>) (N = 8 for each group), were individually housed in metabolic cages for 24 hours, then 4 animals per group were subjected to water deprivation for 24 hours, while 4 animals had free access to water (basal). The 24-hour urine output (A) and urine osmolality (B) of control animals were set as 100%. Urine output of water-deprived animals was reduced of 32% in  $\beta_3$ -AR<sup>+/+</sup> mice and of 40% in  $\beta_3$ -AR<sup>-/-</sup> mice. Urine osmolality of water-deprived animals was increased of 27% in  $\beta_3$ -AR<sup>+/+</sup> mice and of 28% in  $\beta_3$ -AR<sup>-/-</sup> mice. Data are provided as mean  $\pm$  SEM. Significant differences between means were tested by one-way analysis of variance ANOVA with Newman-Keuls's post-test. \*\**P* < 0.001, \**P* < 0.05. No significant interstrain differences were observed. Urine output (C) and natriuresis (D) after the i.p. injection of vehicle or 40 mg/kg bumetanide for 4 hours in  $\beta_3$ -AR<sup>+/+</sup> and  $\beta_3$ -AR<sup>-/-</sup> mice. The 4-hour urine output and urine Na<sup>+</sup> excretion of control animals was set as 100% (n = 5). Data are provided as mean  $\pm$  SEM. Significant differences between means were tested by one-way analysis of variance ANOVA with Newman-Keuls's post-test. \*\*\**P* < 0.0001 for intrastrain differences between vehicle and bumetanide treatments; §*P* < 0.01 for interstrain differences in the effects of bumetanide. The bumetanide-induced natriuresis was significantly attenuated in  $\beta_3$ -AR<sup>-/-</sup> mice compared with  $\beta_3$ -AR<sup>+/+</sup>.

Supplementary material is linked to the online version of the paper at [www.kidney-international.org](http://www.kidney-international.org).

### REFERENCES

- Birnbaumer M, Seibold A, Gilbert S, et al. Molecular cloning of the receptor for human antidiuretic hormone. *Nature*. 1992;357:333-335.

2. Gimenez I, Forbush B. Short-term stimulation of the renal Na-K-Cl cotransporter (NKCC2) by vasopressin involves phosphorylation and membrane translocation of the protein. *J Biol Chem.* 2003;278:26946–26951.
3. Fushimi K, Sasaki S, Yamamoto T, et al. Functional characterization and cell immunolocalization of AQP-CD water channel in kidney collecting duct. *Am J Physiol.* 1994;267:F573–F582.
4. Boone M, Deen PM. Physiology and pathophysiology of the vasopressin-regulated renal water reabsorption. *Pflugers Arch.* 2008;456:1005–1024.
5. Bockenhauer D, Bichet DG. Pathophysiology, diagnosis and management of nephrogenic diabetes insipidus. *Nat Rev Nephrol.* 2015;11:576–588.
6. Bouley R, Hasler U, Lu HA, et al. Bypassing vasopressin receptor signaling pathways in nephrogenic diabetes insipidus. *Semin Nephrol.* 2008;28:266–278.
7. Bouley R, Lu HA, Nunes P, et al. Calcitonin has a vasopressin-like effect on aquaporin-2 trafficking and urinary concentration. *J Am Soc Nephrol.* 2011;22:59–72.
8. Chu JY, Chung SC, Lam AK, et al. Phenotypes developed in secretin receptor-null mice indicated a role for secretin in regulating renal water reabsorption. *Mol Cell Biol.* 2007;27:2499–2511.
9. Jeon US, Joo KW, Na KY, et al. Oxytocin induces apical and basolateral redistribution of aquaporin-2 in rat kidney. *Nephron Exp Nephrol.* 2003;93:e36–e45.
10. Procino G, Milano S, Carmosino M, et al. Combination of secretin and fluvastatin ameliorates the polyuria associated with X-linked nephrogenic diabetes insipidus in mice. *Kidney Int.* 2014;86:127–138.
11. Boivin V, Jahns R, Gambaryan S, et al. Immunofluorescent imaging of beta 1- and beta 2-adrenergic receptors in rat kidney. *Kidney Int.* 2001;59:515–531.
12. Johns EJ, Kopp UC, DiBona GF. Neural control of renal function. *Compr Physiol.* 2011;1:731–767.
13. Mund RA, Frishman WH. Brown adipose tissue thermogenesis: beta3-adrenoceptors as a potential target for the treatment of obesity in humans. *Cardiol Rev.* 2013;21:265–269.
14. Dessy C, Balligand JL. Beta3-adrenergic receptors in cardiac and vascular tissues emerging concepts and therapeutic perspectives. *Adv Pharmacol.* 2010;59:135–163.
15. Chapple CR, Cardozo L, Nitti VW, et al. Mirabegron in overactive bladder: a review of efficacy, safety, and tolerability. *NeuroUrol Urodyn.* 2014;33:17–30.
16. Kaufmann J, Martinka P, Moede O, et al. Noradrenaline enhances angiotensin II responses via p38 MAPK activation after hypoxia/re-oxygenation in renal interlobar arteries. *Acta Physiol (Oxf).* 2015;213:920–932.
17. Rojek A, Nielsen J, Brooks HL, et al. Altered expression of selected genes in kidney of rats with lithium-induced NDI. *Am J Physiol Renal Physiol.* 2005;288:F1276–F1289.
18. Matayoshi T, Kamide K, Takiuchi S, et al. The thiazide-sensitive Na(+)-Cl(-) cotransporter gene, C1784T, and adrenergic receptor-beta3 gene, T727C, may be gene polymorphisms susceptible to the antihypertensive effect of thiazide diuretics. *Hypertens Res.* 2004;27:821–833.
19. Michel-Reher MB, Michel MC. Agonist-induced desensitization of human beta3-adrenoceptors expressed in human embryonic kidney cells. *Naunyn-Schmiedeberg Arch Pharmacol.* 2013;386:843–851.
20. Evans BA, Papaioannou M, Hamilton S, et al. Alternative splicing generates two isoforms of the beta3-adrenoceptor which are differentially expressed in mouse tissues. *Br J Pharmacol.* 1999;127:1525–1531.
21. Mejia R, Wade JB. Immunomorphometric study of rat renal inner medulla. *Am J Physiol Renal Physiol.* 2002;282:F553–F557.
22. Mount DB. Thick ascending limb of the loop of Henle. *Clin J Am Soc Nephrol.* 2014;9:1974–1986.
23. Hebert SC, Culpepper RM, Andreoli TE. NaCl transport in mouse medullary thick ascending limbs. I. Functional nephron heterogeneity and ADH-stimulated NaCl cotransport. *Am J Physiol.* 1981;241:F412–F431.
24. Biner HL, Arpin-Bott MP, Loffing J, et al. Human cortical distal nephron: distribution of electrolyte and water transport pathways. *J Am Soc Nephrol.* 2002;13:836–847.
25. Nielsen S, Chou CL, Marples D, et al. Vasopressin increases water permeability of kidney collecting duct by inducing translocation of aquaporin-CD water channels to plasma membrane. *Proc Natl Acad Sci U S A.* 1995;92:1013–1017.
26. Cernecka H, Sand C, Michel MC. The odd sibling: features of beta3-adrenoceptor pharmacology. *Mol Pharmacol.* 2014;86:479–484.
27. Chijiwa T, Mishima A, Hagiwara M, et al. Inhibition of forskolin-induced neurite outgrowth and protein phosphorylation by a newly synthesized selective inhibitor of cyclic AMP-dependent protein kinase, N-[2-(p-bromocinnamylamino)ethyl]-5-isoquinolinesulfonamide (H-89), of PC12D pheochromocytoma cells. *J Biol Chem.* 1990;265:5267–5272.
28. Gimenez I, Forbush B. Regulatory phosphorylation sites in the NH2 terminus of the renal Na-K-Cl cotransporter (NKCC2). *Am J Physiol Renal Physiol.* 2005;289:F1341–1345.
29. Susulic VS, Frederich RC, Lawitts J, et al. Targeted disruption of the beta 3-adrenergic receptor gene. *J Biol Chem.* 1995;270:29483–29492.
30. Rohrer DK, Chruscinski A, Schauble EH, et al. Cardiovascular and metabolic alterations in mice lacking both beta1- and beta2-adrenergic receptors. *J Biol Chem.* 1999;274:16701–16708.
31. Li JH, Chou CL, Li B, et al. A selective EP4 PGE2 receptor agonist alleviates disease in a new mouse model of X-linked nephrogenic diabetes insipidus. *J Clin Invest.* 2009;119:3115–3126.
32. Strosberg AD, Pietri-Rouxel F. Function and regulation of the beta 3-adrenoceptor. *Trends Pharmacol Sci.* 1996;17:373–381.
33. Pott C, Brixius K, Bundkirchen A, et al. The preferential beta3-adrenoceptor agonist BRL 37344 increases force via beta1-/beta2-adrenoceptors and induces endothelial nitric oxide synthase via beta3-adrenoceptors in human atrial myocardium. *Br J Pharmacol.* 2003;138:521–529.
34. Marples D, Frokiaer J, Dorup J, et al. Hypokalemia-induced downregulation of aquaporin-2 water channel expression in rat kidney medulla and cortex. *J Clin Invest.* 1996;97:1960–1968.
35. Bustamante M, Hasler U, Leroy V, et al. Calcium-sensing receptor attenuates AVP-induced aquaporin-2 expression via a calmodulin-dependent mechanism. *J Am Soc Nephrol.* 2008;19:109–116.
36. Procino G, Carmosino M, Tamma G, et al. Extracellular calcium antagonizes forskolin-induced aquaporin 2 trafficking in collecting duct cells. *Kidney Int.* 2004;66:2245–2255.
37. Silverstein E. Urine specific gravity and osmolality in inbred strains of mice. *J Appl Physiol.* 1961;16:194–196.
38. Claustre Y, Leonetti M, Santucci V, et al. Effects of the beta3-adrenoceptor (Adrb3) agonist SR58611A (amibegron) on serotonergic and noradrenergic transmission in the rodent: relevance to its antidepressant/anti-anxiety-like profile. *Neuroscience.* 2008;156:353–364.
39. Wesche D, Deen PM, Knoers NV. Congenital nephrogenic diabetes insipidus: the current state of affairs. *Pediatr Nephrol.* 2012;27:2183–2204.
40. Moeller HB, Rittig S, Fenton RA. Nephrogenic diabetes insipidus: essential insights into the molecular background and potential therapies for treatment. *Endocr Rev.* 2013;34:278–301.
41. Procino G, Milano S, Carmosino M, et al. Hereditary nephrogenic diabetes insipidus: molecular basis of the defect and potential novel strategies for treatment. *J Genet Syndr Gene Ther.* 2014;5:1000225.
42. Berg T. Altered beta1-3-adrenoceptor influence on alpha2-adrenoceptor-mediated control of catecholamine release and vascular tension in hypertensive rats. *Front Physiol.* 2015;6:120.
43. Loesch A, Unwin R, Gandhi V, et al. Sympathetic nerve varicosities in close apposition to basolateral membranes of collecting duct epithelial cells of rat kidney. *Nephron Physiol.* 2009;113:p15–p21.
44. Abrams P, Kelleher C, Staskin D, et al. Combination treatment with mirabegron and solifenacin in patients with overactive bladder: efficacy and safety results from a randomised, double-blind, dose-ranging, phase 2 study (Symphony). *Eur Urol.* 2015;67:577–588.
45. Cernecka H, Pradidarcheep W, Lamers WH, et al. Rat beta(3)-adrenoceptor protein expression: antibody validation and distribution in rat gastrointestinal and urogenital tissues. *Naunyn-Schmiedeberg Arch Pharmacol.* 2014;387:1117–1127.
46. Sereni F, Dal Monte M, Filippi L, et al. Role of host beta1- and beta2-adrenergic receptors in a murine model of B16 melanoma: functional involvement of beta3-adrenergic receptors. *Naunyn-Schmiedeberg Arch Pharmacol.* 2015;388:1317–1331.
47. Tamma G, Procino G, Strafino A, et al. Hypotonicity induces aquaporin-2 internalization and cytosol-to-membrane translocation of ICln in renal cells. *Endocrinology.* 2007;148:1118–1130.
48. Vrydag W, Michel MC. Tools to study beta3-adrenoceptors. *Naunyn-Schmiedeberg Arch Pharmacol.* 2007;374:385–398.
49. Aragon JP, Condit ME, Bhusan S, et al. Beta3-adrenoceptor stimulation ameliorates myocardial ischemia-reperfusion injury via endothelial nitric oxide synthase and neuronal nitric oxide synthase activation. *J Am Coll Cardiol.* 2011;58:2683–2691.

50. Dal Monte M, Cammalleri M, Mattei E, et al. Protective effects of beta1/2 adrenergic receptor deletion in a model of oxygen-induced retinopathy. *Invest Ophthalmol Vis Sci*. 2014;56:59–73.
51. Dal Monte M, Casini G, Filippi L, et al. Functional involvement of beta3-adrenergic receptors in melanoma growth and vascularization. *J Mol Med*. 2013;91:1407–1419.
52. Hoffmann C, Leitz MR, Oberdorf-Maass S, et al. Comparative pharmacology of human beta-adrenergic receptor subtypes—characterization of stably transfected receptors in CHO cells. *Naunyn-Schmiedeberg Arch Pharmacol*. 2004;369:151–159.
53. Ballester C, Sarria B, Garcia-Granero E, et al. Relaxation by beta 3-adrenoceptor agonists of the isolated human internal anal sphincter. *Life Sci*. 2010;86:358–364.
54. Steinle JJ, Booz GW, Meininger CJ, et al. Beta 3-adrenergic receptors regulate retinal endothelial cell migration and proliferation. *J Biol Chem*. 2003;278:20681–20686.
55. Dal Monte M, Filippi L, Bagnoli P. Beta3-adrenergic receptors modulate vascular endothelial growth factor release in response to hypoxia through the nitric oxide pathway in mouse retinal explants. *Naunyn-Schmiedeberg Arch Pharmacol*. 2013;386:269–278.
56. Wuest M, Eichhorn B, Grimm MO, et al. Catecholamines relax detrusor through beta 2-adrenoceptors in mouse and beta 3-adrenoceptors in man. *J Pharmacol Exp Ther*. 2009;328:213–222.
57. Procino G, Barbieri C, Tamma G, et al. AQP2 exocytosis in the renal collecting duct – involvement of SNARE isoforms and the regulatory role of Munc18b. *J Cell Sci*. 2008;121:2097–2106.
58. Boss O, Bachman E, Vidal-Puig A, et al. Role of the beta(3)-adrenergic receptor and/or a putative beta(4)-adrenergic receptor on the expression of uncoupling proteins and peroxisome proliferator-activated receptor-gamma coactivator-1. *Biochem Biophys Res Commun*. 1999;261:870–876.
59. Ecker PM, Lin CC, Powers J, et al. Effect of targeted deletions of beta1- and beta2-adrenergic-receptor subtypes on heart rate variability. *Am J Physiol Heart Circ Physiol*. 2006;290:H192–H199.
60. Bernstein D, Fajardo G, Zhao M, et al. Differential cardioprotective/ cardiotoxic effects mediated by beta-adrenergic receptor subtypes. *Am J Physiol Heart Circ Physiol*. 2005;289:H2441–H2449.
61. Oppermann M, Mizel D, Kim SM, et al. Renal function in mice with targeted disruption of the A isoform of the Na-K-2Cl co-transporter. *J Am Soc Nephrol*. 2007;18:440–448.